Quantifying the Influence of Atlantic Heat on Barents Sea Ice Variability and Retreat*

M. ÅRTHUN AND T. ELDEVIK

Geophysical Institute, University of Bergen, and Bjerknes Centre for Climate Research, Bergen, Norway

L. H. SMEDSRUD

Uni Research AS, and Bjerknes Centre for Climate Research, Bergen, Norway

Ø. SKAGSETH AND R. B. INGVALDSEN

Institute of Marine Research, and Bjerknes Centre for Climate Research, Bergen, Norway

(Manuscript received 22 August 2011, in final form 6 March 2012)

ABSTRACT

The recent Arctic winter sea ice retreat is most pronounced in the Barents Sea. Using available observations of the Atlantic inflow to the Barents Sea and results from a regional ice–ocean model the authors assess and quantify the role of inflowing heat anomalies on sea ice variability. The interannual variability and longer-term decrease in sea ice area reflect the variability of the Atlantic inflow, both in observations and model simulations. During the last decade (1998–2008) the reduction in annual (July–June) sea ice area was 218×10^3 km^2, or close to 50%. This reduction has occurred concurrent with an increase in observed Atlantic heat transport due to both strengthening and warming of the inflow. Modeled interannual variations in sea ice area between 1948 and 2007 are associated with anomalous heat transport ($r = -0.63$) with a 70×10^3 km^2 decrease per 10 TW input of heat. Based on the simulated ocean heat budget it is found that the heat transport into the western Barents Sea sets the boundary of the ice-free Atlantic domain and, hence, the sea ice extent. The regional heat content and heat loss to the atmosphere scale with the area of open ocean as a consequence. Recent sea ice loss is thus largely caused by an increasing ''Atlantification'' of the Barents Sea.

1. Introduction

The Arctic sea ice cover is a sensitive indicator of climate variability and change (Serreze et al. 2007), and the diminishing Arctic sea ice has had a leading role in recent Arctic temperature amplification (Screen and Simmonds 2010a). In the Barents Sea (Fig. 1a), winter sea ice extent has decreased since 1850 (Shapiro et al. 2003), and the retreat observed during the recent decades (Fig. 2) has been the largest decrease in the Arctic (Parkinson and Cavalieri 2008; Screen and Simmonds 2010b). Variations in the Barents Sea ice extent have been attributed to a number of processes, including large-scale atmospheric circulation anomalies (Maslanik et al. 2007; Deser and Teng 2008; Zhang et al. 2008), cyclone activity (Sorteberg and Kvingedal 2006; Simmonds and Keay 2009), local winds and ice import from the Arctic Ocean (Hilmer et al. 1998; Koenigk et al. 2009; Kwok 2009), and oceanic heat anomalies generated locally (Schlichtholz 2011) or advected into the Barents Sea (Vinje 2001; Kauker et al. 2003; Francis and Hunter 2007).

The Barents Sea has a seasonal ice cover with minimum ice in September and maximum in March/April (Fig. 1a; Kvingedal 2005). Because the majority of the ice is formed locally during winter, Helland-Hansen and Nansen (1909) argued that the sea ice extent in spring is highly dependent on the quantity of heat contained in the water masses of the Barents Sea during winter, and less dependent on variations in air temperature. Anomalous oceanic heat input can thus be reflected downstream by a retreating ice edge (Smedsrud et al. 2010). Interannual variability in Barents Sea ice cover, as well as the negative

* Bjerknes Centre for Climate Research Publication Number A393.

Corresponding author address: M. Årthun, British Antarctic Survey, High Cross, Madingley Road, Cambridge CB3 0ET, United Kingdom.
E-mail: marun@bas.ac.uk

DOI: 10.1175/JCLI-D-11-00466.1

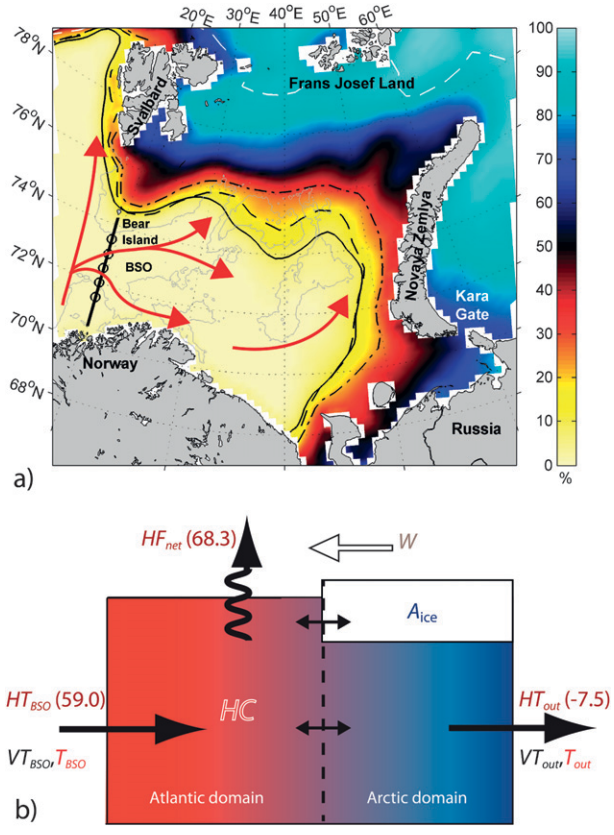

FIG. 1. (a) Satellite-derived (NSIDC) winter (November–April) ice concentration between 1979 and 2010. Winter ice extent (15% concentration) during the 1980s (solid line), 1990s (dashed), and 2000s (dash–dotted) is also shown. The white dashed line is the mean September ice extent during the 1990s. Red arrows indicate main paths of Atlantic water and black circles show mooring locations used to calculate volume and heat transport between Norway and Bear Island [the Barents Sea Opening (BSO)]. (b) Schematic of the Barents Sea long-term mean heat flux, heat transport, and factors related to a variable sea ice area (A_{ice}); HT, VT, and T are the mean heat transport (TW), volume transport, and temperature of the Atlantic inflow (denoted BSO) and the balancing outflow (denoted out; see Table 2 for individual sections), respectively; also, HC is integrated heat content, HF_{net} net heat flux to the atmosphere (in TW), and W is the meridional wind. The sea ice extent defines the boundary between the Atlantic and Arctic domain.

trend, can therefore be understood as a manifestation of the Arcticward extension of the Atlantic domain (i.e., the area where seasonal sea ice formation does not occur; Fig. 1b).

The inflow of Atlantic water between Norway and Bear Island [the Barents Sea Opening (BSO); e.g., Ingvaldsen et al. 2002] is the Barents Sea's main oceanic heat source. The inflow consists of several branches (Fig. 1a; Loeng 1991) but mainly follows a counterclockwise circulation before exiting the Barents Sea between Novaya Zemlya and Franz Josef Land (Schauer et al. 2002). During its passage through the Barents Sea, the Atlantic water loses

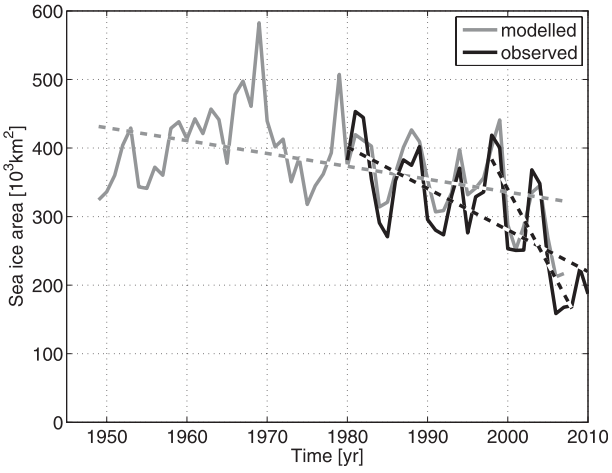

FIG. 2. Annual (July–June) observed (1980–2010) and modeled (1949–2007) sea ice area. Linear trends are shown for 1949–2007 (-19×10^3 km^2 decade^{-1}; modeled), 1980–2010 (-61×10^3 km^2 decade^{-1}; observed), and 1998–2008 (-218×10^3 km^2 decade^{-1}; observed).

most of its heat to the Arctic atmosphere (Häkkinen and Cavalieri 1989; Årthun and Schrum 2010), and the heat transport through the northern exit is consequently small (Gammelsrød et al. 2009). The dominant role of the Atlantic inflow on the Barents Sea heat budget and its intimate link to surface heat fluxes are further evident from the close correspondence between observed volume transport through the BSO and thermal water mass transformation in the western Barents Sea (Segtnan et al. 2010).

It is well established that thermohaline anomalies are advected from the North Atlantic Ocean toward the Arctic, the Barents Sea included (Furevik 2001; Skagseth et al. 2008; Holliday et al. 2008). In support of ocean advection as a potential driver of sea ice extent variability in the Barents Sea, Vinje (2001) found observed temperature anomalies in the central Norwegian Sea to be significantly correlated with the Barents Sea ice extent with a mean lag of two years.

In this paper observational time series of ocean heat transport through the BSO are for the first time considered in light of observed sea ice variability, thus allowing for a quantitative assessment of the manifestation of "Atlantic heat" in recent sea ice retreat. The observation-based description is subsequently supported, generalized, and further quantified by analyzing output from a regional ice–ocean model.

2. Data and methods

a. Observations

1) SEA ICE

Monthly sea ice area from 1979 to 2010 is estimated from passive microwave satellite data on a 25 km × 25 km

grid [National Snow and Ice Data Center (NSIDC); Cavalieri et al. 1996]. The data are derived from two multichannel microwave sensors, the Scanning Multichannel Microwave Radiometer (SMMR) and Special Sensor Microwave/Imager (SSM/I). The sea ice algorithms and the method used to derive a consistent dataset from the two sensors are described in Cavalieri et al. (1999) and references therein. Results considered herein are based on the area 70°–81°N, 15°–60°E (Fig. 1a).

To describe interannual variability in the Barents Sea ice cover we use winter-centered (July–June) annual mean values for all variables. The use of winter-centered averages is beneficial considering the strong seasonality in sea ice extent in the Barents Sea (Fig. 1a) and can be corroborated by a comparison to seasonal averages, with winter-centered values explaining 92% (observations) and 98% (model) of the total variance in December–February mean sea ice area. Named years denote the winter-centered mean that ends in the respective year (i.e., 2007 represents July 2006 to June 2007).

2) Atlantic inflow

To describe the properties of the inflowing Atlantic Water (AW) we use hydrographic data from a section between Norway and Bear Island (BSO; 71.5°–73.5°N, 20°E; Fig. 1a) that has been sampled since 1977 by the Institute of Marine Research, Norway (IMR). The section is typically surveyed 6 times per year, thus capturing the seasonal cycle (Ingvaldsen et al. 2004a) of the Atlantic inflow. Current meter moorings have also been operated by IMR since September 1997 allowing for calculation of AW ($T > 3$°C, $S > 35$; Ingvaldsen et al. 2004a) volume and heat transport through the BSO. The current meter moorings were deployed every 30 nm from 71.5° to 73.5°N with instruments measuring current velocity and temperature at 50-m depth and 15 m above bottom. The heat transport between 71.25° and 73.75°N was estimated using the velocity normal to assigned rectangles centered around the current meters (see, e.g., Ingvaldsen et al. 2004a). Climatological (1998–2008) values were used for July and August 1997 to enable calculation of a winter-centered annual mean value for 1998.

Ocean heat transport through individual sections (e.g., the BSO) must be calculated relative to a reference temperature (T_{ref}), and the choice of reference temperature is in principle arbitrary. We assume for simplicity $T_{\mathrm{ref}} = 0$°C, as commonly used in the oceanographic community; furthermore, it is a representative value for the cold waters leaving the Barents Sea for the Arctic proper (Schauer et al. 2002; Gammelsrød et al. 2009). A uniquely defined ocean heat budget (independent of T_{ref}) results from the heat convergence of a closed mass budget (Montgomery 1974; Schauer and Beszczynska-Möller 2009) and is presented for the modeled Barents Sea in section 4.

3) Wind

Apart from transporting anomalous atmospheric heat to the Barents Sea, winds can influence the ice extent mainly by three processes: 1) stronger northerly winds increase sea ice transport into the Barents Sea from the Arctic Ocean (Kwok 2009); 2) stronger winds increase turbulent heat fluxes at the surface; and 3) stronger winds from the southwest increase the Atlantic inflow through the BSO (Ingvaldsen et al. 2004b). To consider the influence of wind on the sea ice extent, we thus use the meridional wind component from National Centers for Environmental Prediction (NCEP)–National Center for Atmospheric Research (NCAR) reanalysis data (Kalnay et al. 1996) averaged over the Barents Sea. The spatial resolution of NCEP data is O(200 km) and is sufficient to capture synoptic changes in sea level pressure distribution and associated changes in geostrophic winds (e.g., Deser and Teng 2008).

b. Model

To elucidate further the mechanisms influencing the Barents Sea ice cover we utilize a 1948–2007 simulation with the regional ice–ocean model Hamburg Shelf Ocean Model (HAMSOM; Schrum and Backhaus 1999). The setup for the Barents Sea has a horizontal resolution of 7 km × 7 km. A detailed description of the model setup and evaluation with respect to water mass transformation processes and climatic variability in the Barents Sea is given in Årthun and Schrum (2010) and Årthun et al. (2011). The model was found to produce realistic results for the Barents Sea in general, and essentially to reproduce the observed sea ice area from 1979 to 2007 in particular (Table 1; Fig. 2). Temperature variability in the BSO is also well represented by the model. It is more difficult to evaluate modeled volume and heat transport because of the paucity of observations. The seasonality of Atlantic heat (Fig. 3), characterized by a late winter (April) minimum followed by a gradual increase toward early winter, is reproduced by the model, except for higher modeled heat transports during autumn. This season coincides with the maximum strength of the Norwegian Coastal Current (Skagseth et al. 2011), which is not fully captured by the monitoring array. Restricting heat transport calculations to model grid points corresponding to mooring positions and to AW only leads to a more adequate model–observations comparison (Fig. 3). Observed and modeled annual time series have similar mean values (49 and 46 TW, respectively) and magnitude of variability (one standard deviation: 12 and 8 TW, respectively). The net heat transport for the whole

TABLE 1. Maximum lagged (@; lag in number of years) correlations between winter–centered (July–June) annual mean sea ice area ($A_{O,M}$; 70°–81°N, 15°–60°E), and observed (X_O) and modeled (X_M) potential drivers of variability. A positive lag means that sea ice lags. Correlations between observed and modeled parameters are also included. Correlations including observations are done for the common time period for the series in question, whereas model correlations are for the years 1949–2007. To compare with observations, VT_{BSO} and HT_{BSO} were calculated using the spatial resolution of the moorings. Correlations are significant at the 95% confidence level. Asterisk refers to correlations not significant at the 95% confidence level due to the shortness of the observed VT_{BSO} and HT_{BSO} time series. Correlations were calculated after removing linear trends and autocorrelation has been accounted for by adjusting the effective number of independent observations accordingly (Chelton 1983).

	A_{ice}	HT_{BSO}	VT_{BSO}	T_{BSO}	W	HC	HF_{net}	HF_{out}
$r(X_O, A_O)$	1	0.55 @ 2*	−0.50 @ 2*	−0.69 @ 1	0.54 @ 1	—	—	—
$r(X_M, A_M)$	1	−0.63 @ 1	−0.52 @ 0	−0.74 @ 0	0.55 @ 1	−0.86 @ 0	−0.50 @ −1	−0.62 @ −1
$r(X_O, X_M)$	0.91	0.57*	0.49*	0.88	1	—	—	—

BSO (59 TW; Fig. 1) is also in agreement with other recent simulations (e.g., Aksenov et al. 2010). This gives confidence in the model's ability to adequately simulate the inflow of Atlantic heat, and thus to elaborate the causal relationships suggested by the observations.

3. Results

The average observed AW heat transport through the BSO (HT_{BSO}) between 1998 and 2008 is 49 TW with respect to 0°C, ranging between 30 TW in 2001 and 76 TW in 2006. Positive annual heat anomalies coincide with reduced sea ice area (A_{ice}; Fig. 4a), and vice versa. Note that correlations relating to observed heat and volume transport (Table 1) are only considered indicative given the shortness of the time series. Change in volume transport (VT_{BSO}) is the major contributor to observed heat transport variability during this period (Fig. 4a). AW temperatures (T_{BSO}) are, however, strongly correlated to sea ice area between 1979 and 2008 (Fig. 4b, Table 1; Schlichtholz 2011). This is also the case for the longer simulated time series. The recent trend in sea ice area (1998–2008; Fig. 2) corresponds to a reduction of 145×10^3 km^2 per 10 TW of additional Atlantic heat input (Fig. 4a). The increased heat transport is caused by a simultaneous strengthening and warming of the BSO inflow (Fig. 4a; Skagseth et al. 2008).

The longer-term (1980–2009) linear trends in observed inflow temperature and sea ice area are also comparable (Fig. 4b). The trend in sea ice area is -58×10^3 km^2 decade^{-1}, and the observed temperature trend is 0.4°C decade^{-1}. Notably, there is only a relatively weak trend in the meridional wind speed (W) in the Barents Sea. The interannual correlation between wind and sea ice area, on the other hand, is high (Table 1). For example, an event of high annual inflow of sea ice between Svalbard and Franz Josef Land occurred in 2002/03 (141×10^3 km^2) associated with a deep atmospheric low over the eastern Barents Sea (Kwok 2009) and thus anomalous strong northerly winds (Fig. 4b). Ice export from the Arctic contributes 12% (37×10^3 km^2; Kwok 2009) of the annual mean sea ice area in the Barents Sea. However, the lagged response of sea ice area to wind indicates that variation in meridional wind speed influences the Barents Sea ice mainly through its effect on ocean circulation, rather than by the direct influence of anomalous winds on sea ice import. At monthly resolution (not shown) the maximum correlation is found with the sea ice area lagging wind variations by 8 months. Presummer atmospheric forcing is thus important to the sea ice area the following winter, in agreement with Schlichtholz (2011).

The distinct trend in BSO heat transport (Fig. 4a) and temperature (Fig. 4b), and the more modest trend for the local Barents Sea winds, suggests that ocean heat transport is the major player of the two in driving the observed sea ice reduction. The influence of anomalous Atlantic heat on the Barents Sea ocean climate and sea ice area can be further evaluated using the regional ocean model. Consistent lead–lag relationships between

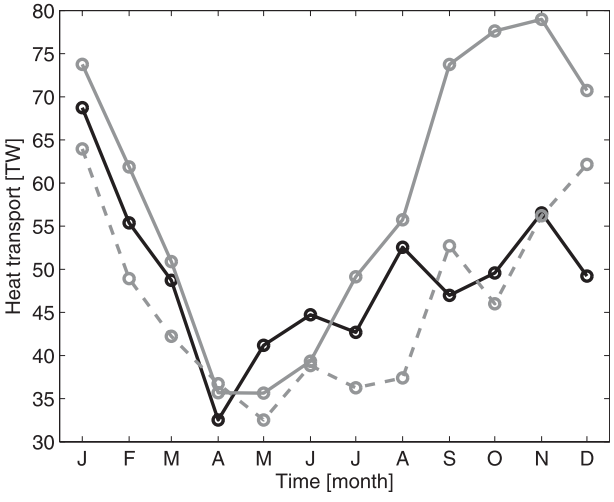

FIG. 3. Seasonal cycle of observed (black solid line) and modeled (gray solid line) BSO heat transport between 1998 and 2007. Dashed line shows modeled heat transport calculated using the spatial resolution of the moorings (cf. text).

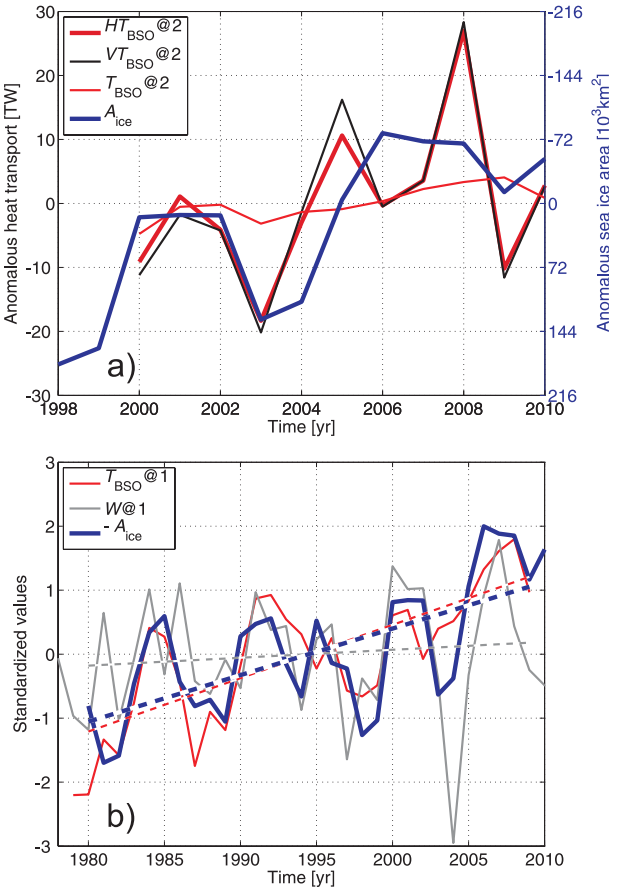

FIG. 4. Observed annual time series of anomalies relevant for Barents Sea ice variability. (a) Anomalous BSO heat transport (HT_{BSO}; dark red) leading the response in sea ice area (A_{ice}, inverted; blue) by two years (@; lag in number of years). The black and red lines are the contributions to HT from anomalous BSO volume transport (VT_{BSO}) and temperature (T_{BSO}), respectively. The scaling of A_{ice} associates a heat loss of 138 W m^{-2} with anomalous loss of sea ice area (q_0 in Fig. 5). (b) Standardized observed BSO temperature, southerly winds (W; gray), and sea ice area (inverted). Temperature and wind lead sea ice area by 1 yr.

observations and model results (Table 1) provide confidence in that the model can be used to explain to what extent anomalous inflow properties are manifested in the interior Barents Sea downstream.

4. Discussion

The influence of anomalous inflow properties on the Barents Sea ocean climate and sea ice area is evaluated by the simulated ocean heat budget. The heat balance in the Barents Sea is predominantly between the ocean heat transport, the rate of change in ocean heat content, and surface heat fluxes (Fig. 1b). There is also a contribution from fluxes due to thermodynamic changes in sea ice thickness not considered herein. The oceanic heat

TABLE 2. Modeled volume (VT) and heat transports (HT) into the Barents Sea. Positive values are defined as eastward and northward. Heat transports are calculated with a reference temperature of 0°C. Note that the net heat transport does not depend on the choice of reference temperature as it is calculated over a closed volume budget.

	Volume transport (Sv)		Heat transport (TW)	
Section	Mean	Std	Mean	Std
BSO	2.3	0.4	59.0	10.6
Franz Josef Land–Novaya Zemlya	1.8	0.4	−2.7	3.9
Svalbard–Franz Josef Land	0.3	0.3	−2.5	1.4
Svalbard–Bear Island	0.0	0.1	−2.0	0.4
Kara Gate	0.2	0.1	−0.2	0.2
Net	0.0	0.6	66.5	11.0

transport to the Barents Sea is essentially provided through the BSO (Table 2). Heat transports through the other gateways are more than an order of magnitude less (with respect to T_{ref}), and the magnitude of variability (standard deviation) is also smaller in the outflow sections. In total, the BSO heat transport carries 79% of the variance in the net advective heat convergence in the Barents Sea (94% if monthly values are considered). For the purpose of understanding the influence of oceanic heat on sea ice variations, it is thus justified to consider only the Atlantic inflow in the BSO.

Positive BSO heat transport anomalies are associated with an increased Barents Sea heat content (HC; quantified as mean temperature) and a reduced sea ice area (Fig. 5). The heat content lags the inflow with one year; there is thus a simultaneous response of the sea ice area and heat content on interannual time scale. Heat loss to the atmosphere (HF_{net} = SW + LW + SE + LA and HF_{out} = HF_{net} − SW, where SW, LW, SE, and LA are shortwave, longwave, sensible, and latent heat fluxes at the ocean surface, respectively) responds thereafter to changes in sea ice area with a 1-yr delay (@ −1 in Table 1, where @ refers to lag). Most of this response is not through stronger heat loss per area of open water, but simply from the increased area over which the heat loss occurs (smaller A_{ice}). This is illustrated in Fig. 5 by scaling the anomalous sea ice area by the heat loss to the atmosphere associated with a variable sea ice cover, quantified as q_0 = std(HF_{net})/std(A_{ice}) = 138 W m^{-2}. A strong spatial correspondence in Arctic sea ice concentration and ocean surface heat fluxes was also found in Screen and Simmonds (2010b). They also argued that the increased oceanic heat loss is likely a response to sea ice loss but did not investigate the causes of the reductions in sea ice. Our lead–lag analysis shows that the sea ice loss links directly to the anomalous Atlantic heat

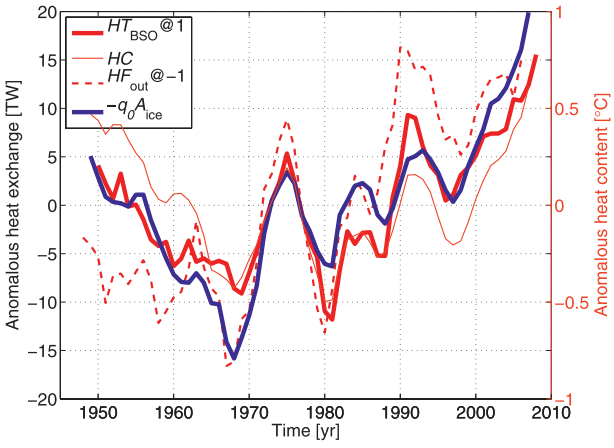

FIG. 5. The modeled lagged (@; lag in number of years) response of Barents Sea ice area (A_{ice}; inverted), HC (quantified as a mean temperature), and oceanic heat loss (HF_{out}: sum of turbulent heat fluxes and longwave radiation) to BSO heat transport (HT_{BSO}). Time series are 5-yr running averages, and q_0 is a constant scaling factor which associates oceanic heat loss with variable sea ice cover (cf. section 4).

input (HT_{BSO}); the ratio of standardized anomalies in A_{ice} to HT_{BSO} (70×10^3 km^2 retreat to 10-TW heat input), which associates an oceanic heat loss essentially equal to q_0. Consequently, the regional heat content and heat loss scale with the area of open ocean.

Temperature and volume transport explain 35% and 70% of the total variance in simulated BSO heat transport, respectively. Despite the limited contribution to variations in Atlantic heat, there is a strong covariability between AW temperatures and sea ice area anomalies (Table 1; see also Schlichtholz 2011). Ice melt is due to a net heat gain to the ice. This heat comes from below as oceanic heat and from above, where solar radiation during summer plays a major role (Sandø et al. 2010). Following Rudels et al. (1999), the fraction of oceanic heat loss that goes into ice melt is proportional to the temperature of the water. This implies not only that a warmer Atlantic inflow increases sea ice melt and thereby the area of open water via its influence on heat transport, but also that more of the heat lost from the AW is going to ice melt, consistent with the relatively high correlation between T and A_{ice} (Table 1).

The lag between temperature variations in the BSO and heat content/sea ice area is related to the residence time of the Barents Sea throughflow (Årthun and Schrum 2010). Additionally, because of substantially stronger heat transports during winter than summer (Fig. 3), the Barents Sea temperature level for the rest of the year is determined by the winter temperatures (Ottersen et al. 2000). There is thus a considerable autocorrelation in temperature between winter and the following summer, leading also to correlations between summer temperature anomalies and sea ice area (e.g., Schlichtholz 2011).

The linear trend in modeled annual sea ice area between 1979 and 2007 (148×10^3 km^2 lost) corresponds to an increase in the open ocean area from 70% to 80% of the total Barents Sea area of 1.4×10^6 km^2. Considering winter (November–April; Fig. 1a) sea ice retreat only, the available cooling area increases from 60% to 72%. This is associated with an increase of the annual mean heat transport by 20 TW (Fig. 5) and a concurrent increase in heat content of 0.9°C in terms of mean temperature. Changes in sea ice area, both interannual (comparing standard deviations) and the long-term trend, thus correspond to about 70×10^3 km^2 retreat with 10 TW of additional heat. This is consistent with Smedsrud et al. (2010), who, using a column model, estimated that an increased oceanic heat transport of 13 TW and 0.8°C increase in mean temperature correspond to a 10% increase in open ocean area. The modeled increase in heat transport is partitioned into a 1.0°C warming of the inflowing water, consistent with the observed temperature increase (Fig. 4b), and a 0.4-Sv (1 Sv $\equiv 10^6$ m^3 s^{-1}) increase in volume transport, corresponding to 53% and 42% of the heat transport increase, respectively (the residual stems from eddy heat transport; $\mathrm{VT}' \times T'$).

The largest retreat in sea ice extent (15% concentration) has occurred in the central and eastern Barents Sea (Fig. 1a), where the hydrography is dominated by the northward flowing AW (Loeng 1991). The increased Atlantic heat leads to a warmer ocean column, thus taking longer to cool to the freezing point during autumn. The area where winter sea ice does not develop has therefore increased. The ice edge has retreated about 240 km at 40°E. The reduction is less pronounced close to Svalbard in the west and to Novaya Zemlya in the east. The latter is most likely due to the topographic control of the Atlantic flow in the eastern Barents Sea (Ozhigin et al. 2000), and the fresh Novaya Zemlya Coastal Current, suggested by Rudels (1987) to be the cause of early sea ice formation west of Novaya Zemlya. The western Barents Sea is to a larger extent influenced by Arctic waters (Pfirman et al. 1994) protecting it from the warmer AW. Thus, in this region the ice extent remains stable.

Warming trends similar to those observed in the BSO (Fig. 4b) have been observed both in the West Spitsbergen Current (Walczowski and Piechura 2006) and upstream in the Norwegian Atlantic Current (Orvik and Skagseth 2005; Skagseth et al. 2008), consistent with an advective signal (Furevik 2001; Holliday et al. 2008). Oceanic heat anomalies in the Barents Sea can also be generated locally by air–sea interaction (Furevik 2001; Schlichtholz and Houssais 2011). We find that the ocean

heat transport through the BSO consistently leads the air–sea fluxes (Fig. 5), indicating advection as a major factor in driving recent sea ice reduction.

5. Conclusions

Sea ice responds to anomalous heating both from below and above and is therefore a sensitive indicator of ongoing climate change. The winter sea ice edge in the eastern Barents Sea has retreated about 240 km during the last three decades (Fig. 1a), and the sea ice area has reached the lowest levels for the last 60 years (Fig. 2). This decrease of sea ice reflects variations in Atlantic heat transport through the Barents Sea Opening, both interannually ($r = -0.63$; Table 1) and for trends both in the short observational record (145×10^3 km^2 per 10 TW; Fig. 4a) and the extended model period (70×10^3 km^2 per 10 TW between 1979 and 2007; Fig. 5).

Complementing the available observations, we have used a regional ice–ocean model to calculate consistent long-term means of Barents Sea ocean heat transport and surface heat fluxes. Keeping in mind that the retreating Barents Sea ice cover is more about the Arcticward expansion of the ice-free region (no wintertime freezing) than the melting of multiyear ice, our study supports the following simple relation between oceanic heat contributed by the Atlantic inflow and sea ice area. The variable heat transport (the ''faucet'') maintains the Atlantic domain of the Barents Sea (the ''warm pool''). This is manifested in the extent of the ice-free region the following year.

The Barents Sea has been in a warm state during the last decades associated with a warm and strong Atlantic inflow (Skagseth et al. 2008). Inflow temperatures, however, have decreased since 2006 (Fig. 4b), 2009 and 2010 included (Karaseva et al. 2010). Consistently, the sea ice area has slightly increased during the same period. This suggests that some recovery of the Barents Sea winter sea ice area may occur in the short term, but if the general positive trend in Atlantic heat input remains, winter cooling will likely be insufficient to produce ice over an increasing area, leading to further ''Atlantification'' of the Barents Sea.

Acknowledgments. This research was supported by the Research Council of Norway through the project IPY–BIAC and by the Centre for Climate Dynamics at the Bjerknes Centre. We thank two anonymous reviewers for constructive suggestions that improved the manuscript, and Corinna Schrum for modelling assistance.

REFERENCES

Aksenov, Y., S. Bacon, A. C. Coward, and A. J. G. Nurser, 2010: The North Atlantic inflow to the Arctic Ocean: High-resolution model study. *J. Mar. Syst.,* **79,** 1–22.

Årthun, M., and C. Schrum, 2010: Ocean surface heat flux variability in the Barents Sea. *J. Mar. Syst.,* **83,** 88–98.

——, R. B. Ingvaldsen, L. H. Smedsrud, and C. Schrum, 2011: Dense water formation and circulation in the Barents Sea. *Deep-Sea Res. I,* **58,** 801–817.

Cavalieri, D. J., C. L. Parkinson, P. Gloersen, and H. J. Zwally, cited 1996: Sea ice concentrations from Nimbus-7 SMMR and DMSP SSM/I passive microwave data. Digital media, National Snow and Ice Data Center. [Available online at http://nsidc.org/data/nsidc-0051.html.]

——, ——, ——, J. C. Comiso, and H. J. Zwally, 1999: Deriving long-term time series of sea ice cover from satellite passive-microwave multisensor data sets. *J. Geophys. Res.,* **104** (C7), 15 803–15 814.

Chelton, D. B., 1983: Effects of sampling errors in statistical estimation. *Deep-Sea Res.,* **30,** 1083–1103.

Deser, C., and H. Teng, 2008: Evolution of Arctic sea ice concentration trends and the role of atmospheric circulation forcing, 1979–2007. *Geophys. Res. Lett.,* **35,** L02504, doi:10.1029/2007GL032023.

Francis, J. A., and E. Hunter, 2007: Drivers of declining sea ice in the Arctic winter: A tale of two seas. *Geophys. Res. Lett.,* **34,** L17503, doi:10.1029/2007GL030995.

Furevik, T., 2001: Annual and interannual variability of the Atlantic Water temperatures in the Norwegian and Barents Seas: 1980–1996. *Deep-Sea Res. I,* **48,** 383–404.

Gammelsrød, T., Ø. Leikvin, V. Lien, W. P. Budgell, H. Loeng, and W. Maslowski, 2009: Mass and heat transports in the NE Barents Sea: Observations and models. *J. Mar. Syst.,* **75,** 56–69.

Häkkinen, S., and D. J. Cavalieri, 1989: A study of oceanic surface heat fluxes in the Greenland, Norwegian, and Barents Sea. *J. Geophys. Res.,* **94** (C5), 6145–6157.

Helland-Hansen, B., and F. Nansen, 1909: The Norwegian Sea. *Fiskdir. Skr. Ser. Havunders.,* **11** (2), 1–360. [Available online at http://web.gfi.uib.no/The%20Norwegian%20Sea/TNS-001.htm.]

Hilmer, M., M. Harder, and P. Lemke, 1998: Sea ice transport: A highly variable link between Arctic and North Atlantic. *Geophys. Res. Lett.,* **25** (17), 3359–3362.

Holliday, N. P., and Coauthors, 2008: Reversal of the 1960s to 1990s freshening trend in the northeast North Atlantic and Nordic Seas. *Geophys. Res. Lett.,* **35,** L03614, doi:10.1029/2007GL032675.

Ingvaldsen, R., H. Loeng, and L. Asplin, 2002: Variability in the Atlantic inflow to the Barents Sea based on a one-year time series from moored current meters. *Cont. Shelf Res.,* **22,** 505–519.

——, L. Asplin, and H. Loeng, 2004a: The seasonal cycle in the Atlantic transport to the Barents Sea during the years 1997–2001. *Cont. Shelf Res.,* **24,** 1015–1032.

——, ——, and ——, 2004b: Velocity field of the western entrance to the Barents Sea. *J. Geophys. Res.,* **109,** C03021, doi:10.1029/2003JC001811.

Kalnay, E., and Coauthors, 1996: The NCEP/NCAR 40-Year Reanalysis Project. *Bull. Amer. Meteor. Soc.,* **77,** 437–471.

Karaseva, T., and Coauthors, 2010: Survey report from the joint Norwegian/Russian ecosystem survey in the Barents Sea August–October 2009. IMR/PINRO Joint Report Series, No. 2/2010, 126 pp. [Available online at http://www.imr.no/filarkiv/2010/09/imr-pinro_2-2010_til_web.pdf/en.]

Kauker, F., R. Gerdes, M. Karcher, C. Köberle, and J. L. Lieser, 2003: Variability of Arctic and North Atlantic sea ice: A combined analysis of model results and observations from 1978 to 2001. *J. Geophys. Res.,* **108,** 3182, doi:10.1029/2002JC001573.

Koenigk, T., U. Mikolajewicz, J. H. Jungclaus, and A. Kroll, 2009: Sea ice in the Barents Sea: Seasonal to interannual variability and climate feedbacks in a global coupled model. *Climate Dyn.,* **32,** 1119–1138.

Kvingedal, B., 2005: Sea-ice extent and variability in the Nordic Seas, 1967–2002. *The Nordic Seas: An Integrated Perspective, Geophys. Monogr.,* Vol. 158, Amer. Geophys. Union, 137–156.

Kwok, R., 2009: Outflow of Arctic Ocean sea ice into the Greenland and Barents Seas: 1979–2007. *J. Climate,* **22,** 2438–2457.

Loeng, H., 1991: Features of the physical oceanographic conditions of the Barents Sea. *Polar Res.,* **10,** 5–18.

Maslanik, J., S. Drobot, C. Fowler, W. Emery, and R. Barry, 2007: On the Arctic climate paradox and the continuing role of atmospheric circulation in affecting sea ice conditions. *Geophys. Res. Lett.,* **34,** L03711, doi:10.1029/2006GL028269.

Montgomery, R. B., 1974: Comments on ''Seasonal variability of the Florida Current,'' by Niiler and Richardson. *J. Mar. Res.,* **32,** 533–535.

Orvik, K. A., and Ø. Skagseth, 2005: Heat flux variations in the eastern Norwegian Atlantic Current toward the Arctic from moored instruments, 1995–2005. *Geophys. Res. Lett.,* **32,** L14610, doi:10.1029/2005GL023487.

Ottersen, G., B. Ådlandsvik, and H. Loeng, 2000: Predicting the temperature of the Barents Sea. *Fish. Oceanogr.,* **9,** 121–135.

Ozhigin, V. K., A. G. Trofimov, and V. A. Ivshin, 2000: The Eastern Basin Water and currents in the Barents Sea. *Proc. ICES Annual Sci. Conf. 2000,* Bruges, Belgium, International Council for the Exploration of the Sea, L14. [Available online at http://www.ices.dk/products/CMdocs/2000/L/L1400.pdf.]

Parkinson, C. L., and D. J. Cavalieri, 2008: Arctic sea ice variability and trends, 1979–2006. *J. Geophys. Res.,* **113,** C07003, doi:10.1029/2007JC004558.

Pfirman, S. L., D. Bauch, and T. Gammelsrød, 1994: The Northern Barents Sea: Water mass distribution and modification. *The Polar Regions and Their Role in Shaping the Global Environment, Geophys. Monogr.,* Vol. 85, Amer. Geophys. Union, 77–94.

Rudels, B., 1987: On the mass balance of the Polar Ocean, with special emphasis on the Fram Strait. *Skr. Nor. Polarinst.,* **188,** 1–35.

——, H. Friedrich, D. Hainbucher, and G. Lohmann, 1999: On the parameterisation of oceanic sensible heat loss to the atmosphere and to ice in an ice-covered mixed layer in winter. *Deep-Sea Res. II,* **46,** 1385–1425.

Sandø, A. B., J. E. Ø. Nilsen, Y. Gao, and K. Lohmann, 2010: Importance of heat transports and local air-sea heat fluxes for Barents Sea climate variability. *J. Geophys. Res.,* **115,** C07013, doi:10.1029/2009JC005884.

Schauer, U., and A. Beszczynska-Möller, 2009: Problems with estimation and interpretation of oceanic heat transport—Conceptual remarks for the case of Fram Strait in the Arctic Ocean. *Ocean Sci.,* **5,** 487–494.

——, H. Loeng, B. Rudels, V. K. Ozhigin, and W. Dieck, 2002: Atlantic Water flow through the Barents and Kara Seas. *Deep-Sea Res. I,* **49,** 2281–2298.

Schlichtholz, P., 2011: Influence of oceanic heat variability on sea ice anomalies in the Nordic Seas. *Geophys. Res. Lett.,* **38,** L05705, doi:10.1029/2010GL045894.

——, and M. N. Houssais, 2011: Forcing of oceanic heat anomalies by air–sea interactions in the Nordic Seas area. *J. Geophys. Res.,* **116,** C01006, doi:10.1029/2009JC005944.

Schrum, C., and J. O. Backhaus, 1999: Sensitivity of atmosphere–ocean heat exchange and heat content in the North Sea and the Baltic Sea. *Tellus,* **51,** 526–549.

Screen, J. A., and I. Simmonds, 2010a: The central role of diminishing sea ice in recent Arctic temperature amplification. *Nature,* **464,** 1334–1337.

——, and ——, 2010b: Increasing fall-winter energy loss from the Arctic Ocean and its role in Arctic temperature amplification. *Geophys. Res. Lett.,* **37,** L16707, doi:10.1029/2010GL044136.

Segtnan, O. H., T. Furevik, and A. D. Jenkins, 2010: Computing cross-isotherm volume transports from ocean temperature observations and surface heat fluxes, with application to the Barents Sea inflow. *Cont. Shelf Res.,* **30,** 1830–1839.

Serreze, M. C., M. M. Holland, and J. Stroeve, 2007: Perspectives on the Arctic's shrinking sea-ice cover. *Science,* **315,** 1533–1536.

Shapiro, I., R. Colony, and T. Vinje, 2003: April sea ice extent in the Barents Sea, 1850–2001. *Polar Res.,* **22,** 5–10.

Simmonds, I., and K. Keay, 2009: Extraordinary September Arctic sea ice reductions and their relationships with storm behavior over 1979–2008. *Geophys. Res. Lett.,* **36,** L19715, doi:10.1029/2009GL039810.

Skagseth, Ø., T. Furevik, R. Ingvaldsen, H. Loeng, K. A. Mork, K. A. Orvik, and V. Ozhigin, 2008: Volume and heat transports to the Arctic Ocean via the Norwegian and Barents Seas. *Arctic Subarctic Ocean Fluxes: Defining the Role of the Northern Seas in Climate,* R. Dickson, J. Meincke, and P. Rhines, Eds., Springer, 45–64.

——, K. F. Drinkwater, and E. Terrile, 2011: Wind- and buoyancy-induced transport of the Norwegian Coastal Current in the Barents Sea. *J. Geophys. Res.,* **116,** C08007, doi:10.1029/2011JC006996.

Smedsrud, L. H., R. Ingvaldsen, J. E. Ø. Nilsen, and Ø. Skagseth, 2010: Heat in the Barents Sea: Transport, storage, and surface fluxes. *Ocean Sci.,* **6,** 219–234.

Sorteberg, A., and B. Kvingedal, 2006: Atmospheric forcing on the Barents Sea winter ice extent. *J. Climate,* **19,** 4772–4784.

Vinje, T., 2001: Anomalies and trends of sea-ice extent and atmospheric circulation in the Nordic Seas during the period 1864–1998. *J. Climate,* **14,** 255–267.

Walczowski, W., and J. Piechura, 2006: New evidence of warming propagating toward the Arctic Ocean. *Geophys. Res. Lett.,* **33,** L12601, doi:10.1029/2006GL025872.

Zhang, X., A. Sorteberg, J. Zhang, R. Gerdes, and J. C. Comiso, 2008: Recent radical shifts of atmospheric circulations and rapid changes in Arctic climate system. *Geophys. Res. Lett.,* **35,** L22701, doi:10.1029/2008GL035607.